

Delay time dependence of wave packet motion and population transfer of four-level K_2 molecule in pump-pump-probe pulses

Zhiqiang Chang(常志强), Changming Li(李昌明), Guo Wei(郭玮), Hongbin Yao(姚洪斌)
Citation: Chin. Phys. B . 2018, 27(5): 053301. **doi:** 10.1088/1674-1056/27/5/053301

Journal homepage: http://cpb.iphy.ac.cn; http://iopscience.iop.org/cpb

What follows is a list of articles you may be interested in

Attosecond transient absorption spectroscopy: Comparative study based on three-level modeling

Zeng-Qiang Yang(杨增强), Di-Fa Ye(叶地发), Li-Bin Fu(傅立斌)
Chin. Phys. B . 2018, 27(1): 013301. **doi:** 10.1088/1674-1056/27/1/013301

Frequency dependence of quantum path interference in non-collinear high-order harmonic generation

Shi-Yang Zhong(钟诗阳), Xin-Kui He(贺新奎), Hao Teng(滕浩), Peng Ye(叶蓬), Li-Feng Wang(汪礼锋), Peng He(何鹏), Zhi-Yi Wei(魏志义)
Chin. Phys. B . 2016, 25(2): 023301. **doi:** 10.1088/1674-1056/25/2/023301

Effect of pump-1 laser on Autler–Townes splitting in photoelectron spectrum of K_2 molecule

Guo Wei, Lu Xing-Qiang, Wang Xin-Lin, Yao Hong-Bin
Chin. Phys. B . 2015, 24(1): 013302. **doi:** 10.1088/1674-1056/24/1/013302

Fine-tuning the thicknesses of organic layers to realize high-efficiency and long-lifetime blue organic light-emitting diodes

Yu Jian-Ning, Zhang Min-Yan, Li Chong, Shang Yu-Zhu, Lü Yan-Fang, Wei Bin, Huang Wei
Chin. Phys. B . 2012, 21(8): 083303. **doi:** 10.1088/1674-1056/21/8/083303

Autler–Townes splitting in photoelectron spectra of K_2 molecule

Yao Hong-Bin,Zheng Yu-Jun
Chin. Phys. B . 2012, 21(2): 023302. **doi:** 10.1088/1674-1056/21/2/023302

Delay time dependence of wave packet motion and population transfer of four-level K_2 molecule in pump–pump–probe pulses*

Zhiqiang Chang(常志强)[1], Changming Li(李昌明)[1], Wei Guo(郭玮)[1,2,†], and Hongbin Yao(姚洪斌)[3]

[1] *School of Electrical Engineering, University of South China, Hengyang* 421001, *China*
[2] *State Key Laboratory of Molecular Reaction Dynamics, Dalian Institute of Chemical Physics, Dalian* 116023, *China*
[3] *Key Laboratory of New Energy and Materials, Xinjiang Institute of Engineering, Urumqi* 830091, *China*

(Received 17 January 2018; revised manuscript received 1 March 2018; published online 26 April 2018)

The effect of delay time on photoelectron spectra and state populations of a four-level ladder K_2 molecule is investigated by a pump1–pump2–probe pulse via the time-dependent wave packet approach. The periodical motion of the wave packet leads to the periodical change of the photoelectron spectra. The Autler–Townes triple splitting appears at zero delay time, double splitting appears at nonzero delay time between pump1 and pump2 pulses, and no splitting appears at nonzero delay time between pump2 and probe pulses. The periodical change of the state populations with the delay time may be due to the coupling effect between the two pulses. It is found that the selectivity of the state populations may be attained by regulating the delay time. The results can provide an important basis for realizing the optical control of molecules experimentally.

Keywords: wave packet motion, population transfer, intense femtosecond pump1–pump2–probe pulse, four-level ladder K_2 molecule

PACS: 33.60.+q, 33.20.Xx, 42.50.Hz **DOI:** 10.1088/1674-1056/27/5/053301

1. Introduction

The femtosecond laser can regulate the molecular dynamics in real time. A benefit of light manipulation of molecular processes is controlling the evolution of the wave packet. The photoelectron spectra and state populations map the wave packet dynamics information of the excited state. They were studied in multi-level molecular systems, and were found to be sensitive to the parameters of the laser fields.[1–33]

For an alkali metal dimer, a femtosecond pump–probe pulse can be used for studying the dynamics of the wave packet on the excited state. Braun *et al.*,[1] Miao *et al.*,[2,3] and Liu *et al.*[4] found that the state populations and photoelectron spectra of NaI change with the delay time. Zhao *et al.*[5] studied the sensitivity of the predissociation dynamics of NaI to the field-free orientation. Yu *et al.*[6] studied the effect of the delay time and laser wavelength on the evolution of the wave packet of NaK. The periodical motion of the wave packet leads to the periodical change of the photoelectron spectra. Ma *et al.*[7] found that the wave packet on the excited state moves periodically, the state population of NaRb is affected by the laser intensity. Zhang *et al.*[8,9] suggested that the laser wavelength affects the oscillation period of the wave packet, and the peak positions and heights of the photoelectron spectra of NaLi vary with the delay time. The efficiency of population transfer through diabatic coupling strength changes with the laser intensity and laser wavelength. The delay time alters the peak positions and heights of the photoelectron spectra. Zhu *et al.*[10] presented that the delay time affects the state populations of the CsI molecule. Meng *et al.*[11,12] and Wang *et al.*[13] studied the sensitivity of the state populations of NO to the laser intensity, laser wavelength, pulse width, and delay time, and presented the periodical change with the laser intensity and pulse width. Cheng *et al.*[14] found that the selective excitation of excited states can be achieved by phase modulation. Niu *et al.*[15] proposed that the rovibrational population transfer can be controlled by a two-overlapping-pulse scheme. Xie *et al.*[16] found that the population exchange can occur due to the driving action of an external field.

The dynamics of the wave packet of a homonuclear diatomic molecule shares some similar characteristics with that of a heteronuclear diatomic molecule. The periodical wave packet motion of the four-level Na_2 was studied in Refs. [17]–[19]. Yuan *et al.*[20,21] found that the state populations change with the delay time; the more effective scheme for controlling the population transfer of the three-level Na_2 is the one with a short pulse width and positive delay time, which is explained by the light-induced potentials (LIPs). Hu *et al.*[22] and Yan *et al.*[23] studied the sensitivity of the population transfer and the angular distribution of population of the four-level Li_2 to the molecular rotation. Han *et al.*[24] and Jing *et al.*[25] presented that the laser intensity, wavelength, and delay time affect the state population of the four-level Li_2. Liu *et al.*[26,27] proposed that the delay time only alters the peaks height, but does not

*Project supported by the National Natural Science Foundation of China (Grant Nos. 11704178 and 11764041) and the Scientific Research Fund of Hunan Provincial Education Department, China (Grant No. 15B204).

†Corresponding author. E-mail: vella99@163.com

© 2018 Chinese Physical Society and IOP Publishing Ltd

change the peak positions of the photoelectron spectra of Li_2. Miao *et al.*[28,29] suggested that the peak positions and heights in the photoelectron spectra of I_2^- anion change with the delay time. The total photoelectron signal shows a periodical oscillation with the increase of the delay time.

The Autler–Townes (AT) triple splitting and the selective distributions of the dressed states may be attained by altering the laser intensity, wavelength, and pulse envelope.[30–32] No studies focus on the sensitivity of the wave packet dynamics of the four-level ladder K_2 to the delay time. New data on the delay time dependence of the photoelectron spectra and state populations of the four-level ladder K_2 molecule is obtained in the presence of two control pump fields and one probe field via the time-dependent quantum wave packet method.

2. Theory

Four states (ground state $|\mathrm{X}\rangle\,{}^1\Sigma_g^+$, excited states $|\mathrm{A}\rangle\,{}^1\Sigma_u^+$ and $|2\rangle\,{}^1\Pi_g^+$, and ionic ground state $|\mathrm{X}^+\rangle\,{}^2\Sigma_g^+$, abbreviated to $|\mathrm{X}\rangle$, $|\mathrm{A}\rangle$, $|2\rangle$, and $|\mathrm{X}^+\rangle$, respectively) are included in the ionization of the four-level ladder K_2,[30,34,35] as shown in Fig. 1.

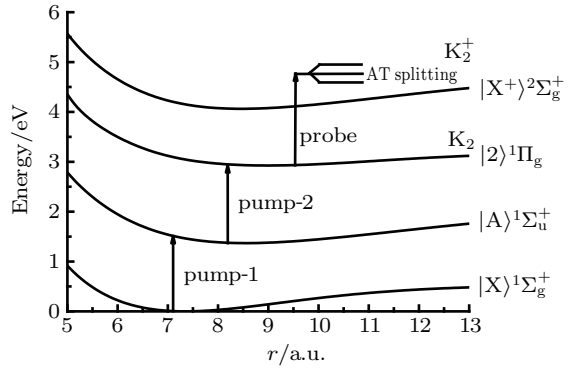


Fig. 1. Potential energy curves of K_2 molecule taken from Refs. [30], [34], and [35].

The wave functions of the three-state model are written in the column vector

$$\boldsymbol{\Psi} = (\psi_\mathrm{X}, \psi_\mathrm{A}, \psi_2, \psi_\mathrm{I})^\mathrm{T}, \tag{1}$$

where ψ_X, ψ_A, ψ_2, and ψ_I are the wave functions of $|\mathrm{X}\rangle$, $|\mathrm{A}\rangle$, $|2\rangle$, and $|\mathrm{X}^+\rangle$, respectively. $|\mathrm{X}^+\rangle$ is a continuum state and can be discretized into a band of quasicontinuum states. The ψ_I is expressed as

$$\psi_\mathrm{I} = \left(\psi^{(1)}, \psi^{(2)}, \ldots, \psi^{(N)}\right)^\mathrm{T}, \tag{2}$$

where N is the number of discrete states of the K_2 ion. The time-dependent Schrödinger equation in the Born–Oppenheimer frame is expressed as

$$\mathrm{i}\hbar\frac{\partial}{\partial t}\begin{pmatrix}\psi_\mathrm{X}\\ \psi_\mathrm{A}\\ \psi_2\\ \psi^{(1)}\\ \psi^{(2)}\\ \vdots\\ \psi^{(N)}\end{pmatrix} = -\frac{\hbar^2}{2\mu}\frac{\partial^2}{\partial r^2}\begin{pmatrix}\psi_\mathrm{X}\\ \psi_\mathrm{A}\\ \psi_2\\ \psi^{(1)}\\ \psi^{(2)}\\ \vdots\\ \psi^{(N)}\end{pmatrix} + \boldsymbol{U}(r,t)\begin{pmatrix}\psi_\mathrm{X}\\ \psi_\mathrm{A}\\ \psi_2\\ \psi^{(1)}\\ \psi^{(2)}\\ \vdots\\ \psi^{(N)}\end{pmatrix}, \tag{3}$$

where $\boldsymbol{U}(r,t)$ is the potential matrix and is given by

$$\boldsymbol{U}(r,t) = \begin{pmatrix} V_\mathrm{X} & W_\mathrm{XA} & 0 & 0 & \cdots & 0\\ W_\mathrm{AX} & V_\mathrm{A} & W_\mathrm{A2} & 0 & \cdots & 0\\ 0 & W_{2A} & V_2 & W_\mathrm{2I} & \cdots & W_\mathrm{2I}\\ 0 & 0 & W_\mathrm{I2} & V_\mathrm{I}+E_{\mathrm{I},1} & \cdots & 0\\ \vdots & \vdots & \vdots & \vdots & \ddots & \vdots\\ 0 & 0 & W_\mathrm{I2} & 0 & \cdots & V_\mathrm{I}+E_{\mathrm{I},N}\end{pmatrix}, \tag{4}$$

where V_X, V_A, V_2, and V_I are the potential energy curves of the four electronic states at zero field. $E_{\mathrm{I},i} = (i-1)\Delta E_\mathrm{I}$ $(i = 1,2,\ldots,N)$ is the emitted photoelectron energy. Other nonzero off-diagonal matrix elements are given by

$$\begin{aligned} W_\mathrm{XA} &= W_\mathrm{AX} = \hbar R_\mathrm{XA}(r)\cos(\omega_1 t)\\ &= \mu_\mathrm{XA}(r)\,e_1 f_1(t)\cos(\omega_1 t), \end{aligned} \tag{5}$$

$$\begin{aligned} W_\mathrm{A2} &= W_{2A} = \hbar R_\mathrm{A2}\cos[\omega_2(t-\Delta t_1)]\\ &= \mu_\mathrm{A2}(r)\,e_2 f_2(t)\cos[\omega_2(t-\Delta t_1)], \end{aligned} \tag{6}$$

$$\begin{aligned} W_\mathrm{2I} &= W_\mathrm{I2} = \hbar R_\mathrm{I2}\cos[\omega_3(t-\Delta t_2)]\\ &= \mu_\mathrm{2I}(r)\,e_3 f_3(t)\cos[\omega_3(t-\Delta t_2)], \end{aligned} \tag{7}$$

$$f_1(t) = \exp\left[-4\ln 2\cdot(t/\tau)^2\right], \tag{8}$$

$$f_2(t) = \exp\left[-4\ln 2\cdot((t-\Delta t_1)/\tau)^2\right], \tag{9}$$

$$f_2(t) = \exp\left[-4\ln 2\cdot((t-\Delta t_2)/\tau)^2\right], \tag{10}$$

where $R_\mathrm{XA}(r)$, $R_\mathrm{A2}(r)$, and $R_\mathrm{2I}(r)$ are the Rabi frequencies, $\mu_\mathrm{XA}(r)$, $\mu_\mathrm{A2}(r)$, and $\mu_\mathrm{2I}(r)$ are the transition dipole moments, e_1, e_2, and e_3 are the amplitudes of the pump and probe laser fields, ω_1, ω_2, and ω_3 the angular frequencies, $f_1(t)$, $f_2(t)$, and $f_3(t)$ are the envelopes, τ is the pulse width, Δt_1 is the delay time between the pump-1 and pump-2 pulses, and Δt_2 is the delay time between the pump-2 and probe pulses.

The split-operator Fourier method is used to solve the time-dependent Schrödinger equation.[29,30] The population on each electronic state is written as[2–13,22,24,25,27,29]

$$P_k(t) = \int |\psi_k(r,t)|^2\,\mathrm{d}r, \quad (k = \mathrm{X},\mathrm{A},2,\mathrm{I}). \tag{11}$$

The photoelectron spectrum is defined as[1,3,4,6,8,22,24,27,29–32]

$$P_i(E_{\mathrm{I},i}) = \lim_{t\to\infty}\int \mathrm{d}r\left|\psi^{(i)}(r,t,E_{\mathrm{I},i})\right|^2, \quad (i = 1,2,\ldots,N). \tag{12}$$

The potential energy curves are taken from Ref. [37]. The transition dipole moments are taken from Ref. [38]. In the calculation, the energy range $E_{\mathrm{I},i}$ spans over 0–1.2 eV and N is taken to be 120.

From the dressed-state theory, the excited state $|2\rangle$ is dressed by the laser field and splits into three substates $|\alpha\rangle$, $|\beta\rangle$, and $|\gamma\rangle$ with energy $V_2+\hbar R/2$, V_2, and $V_2-\hbar R/2$. The wave function of state $|2\rangle$, including the influence of the laser field, can be expressed by dressed states $|\alpha\rangle$, $|\beta\rangle$, $|\gamma\rangle$ whose energies are dressed in order,[25,29]

$$\psi_2(r,t) = A|\alpha\rangle + B|\beta\rangle + C|\gamma\rangle, \tag{13}$$

$$|\alpha\rangle = \exp\left[-\mathrm{i}\left(V_2+\hbar R/2\right)t/\hbar\right]\psi_2(r), \tag{14}$$

$$|\beta\rangle = \exp\left(-\mathrm{i}V_2 t/\hbar\right)\psi_2(r), \tag{15}$$

$$|\gamma\rangle = \exp\left[-\mathrm{i}\left(V_2-\hbar R/2\right)t/\hbar\right]\psi_2(r), \tag{16}$$

where $A=\frac{R_{\mathrm{A2}}}{\sqrt{2}R}$, $B=\frac{R_{\mathrm{XA}}}{R}$, $C=\frac{R_{\mathrm{A2}}}{\sqrt{2}R}$, and $R=\sqrt{R_{\mathrm{XA}}^2+R_{\mathrm{A2}}^2}$.

3. Results and discussion

The delay time dependence of the wave packet motion is studied. Figure 2 displays the evolution of the wave packet on excited states $|A\rangle$ and $|2\rangle$ for two cases: $\Delta t_1 = 2100$ fs with $\Delta t_2 = 0$ fs and $\Delta t_2 = 2100$ fs with $\Delta t_1 = 0$ fs. The wave packet on excited state $|\mathrm{A}\rangle$ moves periodically with roundtrip time 550 fs for the two cases. The periodical motion was not reported before for the four-level ladder K_2, but for other alkali metal dimmers, such as the four-level Na_2,[17,18] NaI,[1] NaK,[6] NaRb,[7] and NaLi.[8,9] The wave packet moves from the inner turning point (7 a.u.) towards the outer turning point (11 a.u.) during 0–275 fs, and reaches the outer turning point at 275 fs. Then the wave packet moves back to the inner turning point during 275–550 fs, and reaches the inner turning point at 550 fs. This is a complete motion within an oscillation period, which leads to the periodical variation of the peak position in the photoelectron spectra with delay time, see Fig. 3. The wave packet on excite state $|2\rangle$ moves periodically with roundtrip time 700 fs only for $\Delta t_2 = 2000$ fs with $\Delta t_1 = 0$, and the oscillation amplitude is 7–12 a.u.

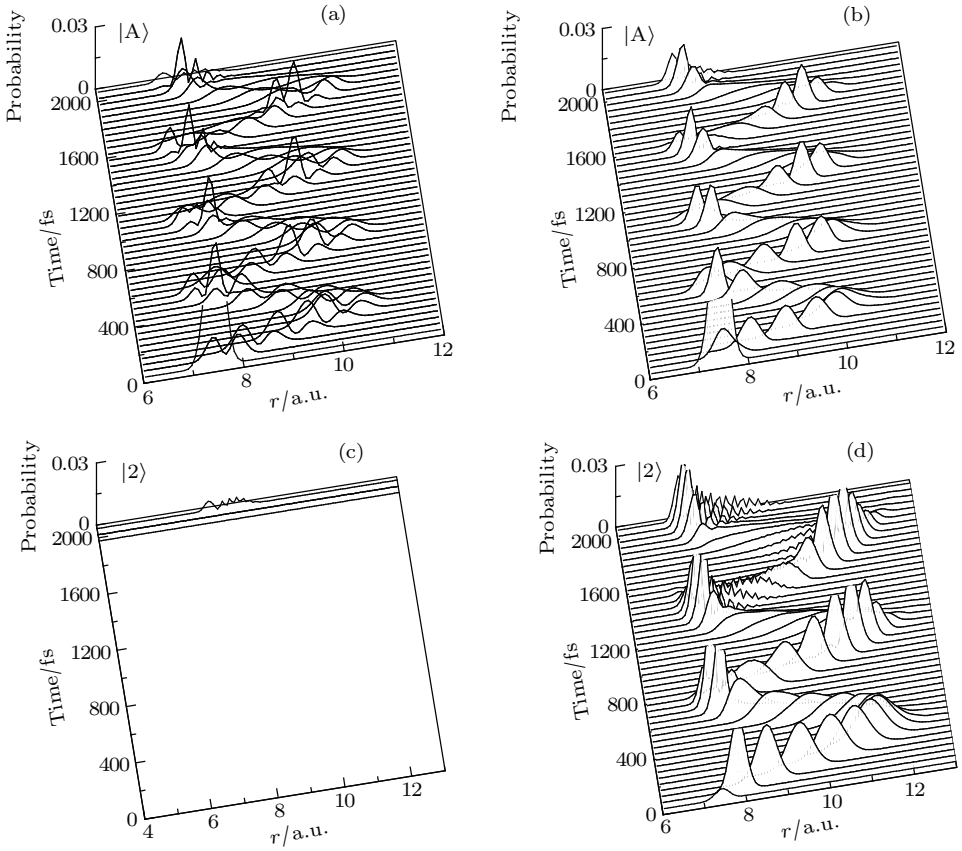


Fig. 2. The evolution of the wave packet on excited states $|\mathrm{A}\rangle$ and $|2\rangle$ with time and internuclear separation: (a) and (c) $\Delta t_1 = 2100$ fs, $\Delta t_2 = 0$ fs, (b) and (d) $\Delta t_1 = 0$ fs, $\Delta t_2 = 2100$ fs. Other laser parameters are $\lambda_1 = 848$ nm, $\lambda_2 = \lambda_3 = 785$ nm, $\tau = 30$ fs, and $I_1 = I_2 = I_3 = 4\times10^{11}$ W/cm^2.

The delay time dependence of the photoelectron spectra is studied. Figure 3 displays the evolution of the photoelectron spectra within the first oscillating period (0–550 fs). Three features can be seen in Fig. 3. Firstly, AT triple splitting with symmetric profiles appears in the photoelectron spectra at zero delay time, which results from the sufficient Rabi oscillation within the resonant region.[39] The symmetric triplet was observed for the four-level Na_2,[40] Li_2,[22,25] and K_2.[30–32] The splitting disappears progressively with the increase of the delay time, and the three peaks transform into double peaks in Fig. 2(a) and into one peak in Fig. 2(b) at 30 fs. The disappearance of AT splitting is due to the non-sufficient Rabi oscillation within the off-resonant region induced by the larger delay time. According to Eq. (13), the probabilities of the cen-

tral peak and two side peaks are determined by R_{XA} and R_{A2}, respectively. The larger Δt_1 lowers R_{XA}, which results in the disappearance of the central peak, while the larger Δt_2 lowers R_{A2}, which results in the disappearance of the two side peaks. Secondly, the peaks shift to lower energy during 0–275 fs while they shift to higher energy during 275–550 fs. The symmetric center is at about 0.484 eV at zero delay time, which is calculated by $E_{v0} + \Sigma\hbar\omega_k - V_I(r)$,[39] where E_{v0} and $V_I(r)$ are the potentials of the vibrational ground state and the ionic state, respectively, and $\hbar\omega_k$ is the photon energy. At zero delay time ($\Delta t_1 = 0$ and $\Delta t_2 = 0$), $V_I(r)$ is the potential of the ionic state at the equilibrium distance r_0 of the neutral ground state, i.e., $V_I(r_0)$. The two side peaks are at $0.484 - R/2$ and $0.484 + R/2$. As the delay time Δt_2 increases from 0 fs to 275 fs, the difference between the potentials of the excited state $|2\rangle$ and ionic state $|X^+\rangle$ increase with the increase of the internuclear separation, leading to the decrease of the photoelectron energy with the increase of the internuclear separation. It is easy to adapt the same procedure to interpret the increase of the photoelectron energy with the decrease of the internuclear separation as the delay time increases from 275 fs to 550 fs, see Fig. 2(b). This was reported before for other alkali metal dimmers four-level Na_2,[17–19] NaI,[1] and NaK,[6] but not for the four-level K_2. Liu *et al.*[26,27] found that the delay time only affects the peak height, but does not affect the peak positions in the photoelectron spectra of four-level Li_2. The different results may be induced by the different pulse widths (260 fs in Refs. [26] and [27] versus 30 fs in this study). The wave packet may almost reside stationarily at the equilibrium position of the excited state potential due to the longer pulse width,[17] which leads to the independence of the peak positions on the delay time. In fact, studies on the periodical variation of the photoelectron spectra are with short pulse width (shorter than 100 fs).[1,6,17–19] Thirdly, the peak height decreases progressively with the increase of the delay time in Fig. 3(a), which indicates the decrease of the amount of emitted photoelectrons with the increase of the delay time (0–550 fs) for $\Delta t_2 = 0$. The peak height decreases and then increases with the increase of the delay time in Fig. 3(b), which indicates that the amount of the emitted photoelectrons decreases and then increases with the increase of the delay time (0–550 fs) for $\Delta t_1 = 0$.

The delay time dependence of the state populations is studied. Figure 4 shows the evolution of the state populations at different delay time for two cases: $\Delta t_1 = 0$–2100 fs with $\Delta t_2 = 0$ (case 1) and $\Delta t_2 = 0$–2100 fs with $\Delta t_1 = 0$ (case 2). Three features are seen in Fig. 4. Firstly, for case 1, the populations on the ground state and excited state $|A\rangle$ take the Rabi oscillation with the pump-1 pulse on. The Rabi oscillation stops when the pump-1 pulse is off. The population on the ground state remains unchanged after the pump-1 pulse disappears. The population on excited state $|A\rangle$ remains unchanged after the pump-1 pulse disappears and before the pump-2 pulse arrives. There is no population on excited state $|2\rangle$ before the pump-2 pulse arrives. The populations on excited states $|A\rangle$and $|2\rangle$ take Rabi oscillation with the pump-2 pulse on. There is no population on the ionic state before the probe pulse arrives. For case 2, the populations on the ground state and excited states take Rabi oscillation with the pump pulses on. The Rabi oscillation stops when the pump pulses disappear. The populations on the ground state and excited state $|A\rangle$ remain unchanged after the pump pulses disappear. The population on excited state $|2\rangle$ remains unchanged after the pump pulses disappear and before the probe pulse arrives. There is no population on the ionic state before the probe pulse arrives. Secondly, the Rabi oscillation becomes weaker as the delay time increases. The disappearance of AT splitting in the photoelectron spectra results from the nonsufficient Rabi oscillation, see Fig. 3. Thirdly, for case 1, the populations on

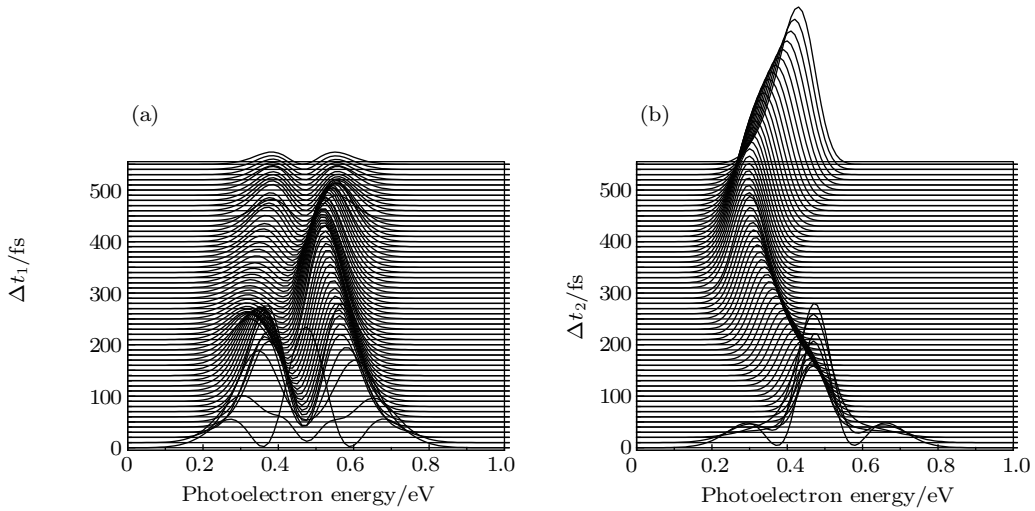


Fig. 3. The evolution of photoelectron spectra of K_2 (a) at different delay time Δt_1 with $\Delta t_2 = 0$ and (b) at different delay time Δt_2 with $\Delta t_1 = 0$. All the other parameters are the same as those in Fig. 2.

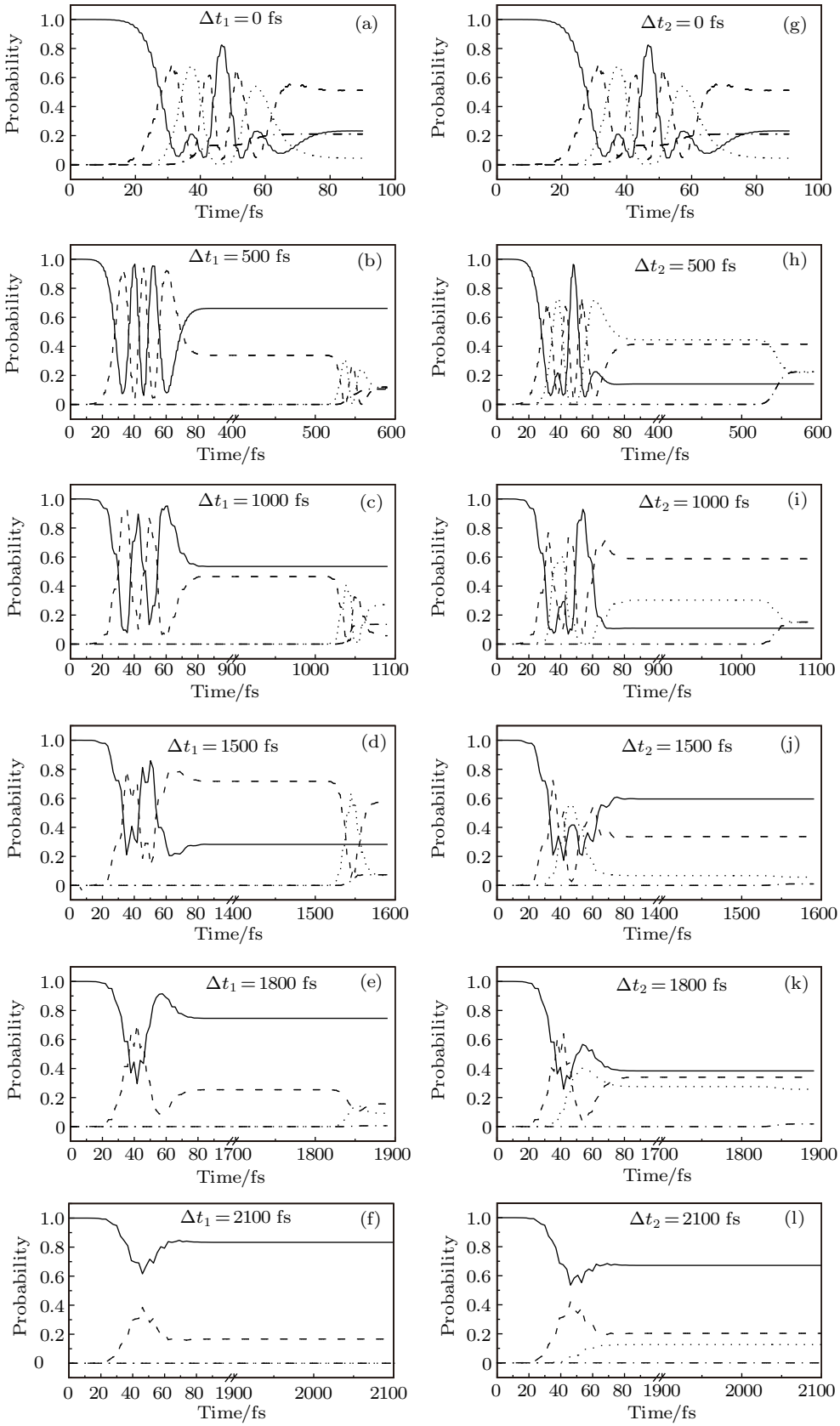


Fig. 4. (color online) The evolution of state populations (a)–(f) at different delay time Δt_1 with $\Delta t_2 = 0$ and (g)–(l) at different delay time Δt_2 with $\Delta t_1 = 0$. The solid, dash, dot, and dash dot represent ground state $|\mathrm{X}\rangle$, excited state $|\mathrm{A}\rangle$, excited state $|2\rangle$ and ionic state $|\mathrm{X}^+\rangle$, respectively. Other laser parameters are the same as those in Fig. 2.

the ground state and excited state $|\mathrm{A}\rangle$ present the periodical change with the increase of the delay time. For case 2, the populations on the ground state and two excited states present the periodical change with the increase of the delay time. The periodical change of the population with the delay time was not studied before for the four-level K_2, and can be interpreted

by the coupling effect between the two pulses. The coupling effect is weakened by the larger delay time. Accordingly, the intensity of the Rabi oscillation is weakened. The different Rabi oscillation results in the different population left on each electronic state.[9]

4. Conclusions

The effect of the delay time (case 1: $\Delta t_1 = 0$–2100 fs and $\Delta t_2 = 0$, case 2: $\Delta t_2 = 0$–2100 fs and $\Delta t_1 = 0$) on the photoelectron spectra and state populations of the four-level ladder K_2 molecule by a pump1–pump2–probe pulse is firstly investigated via the time-dependent wave packet approach. The wave packet on excited state $|A\rangle$ moves periodically with roundtrip time 550 fs and oscillation amplitude 7–11 a.u., while the wave packet on excite state $|2\rangle$ moves periodically with roundtrip time 700 fs and oscillation amplitude 7–12 a.u. only for case 2. The periodical motion of the wave packet leads to the periodical variation of the photoelectron spectra. The photoelectron spectra show AT triple splitting with symmetric profiles at zero delay time. As the delay time increases, the three peaks become double peaks for case 1 and one peak for case 2. The coupling effect is weakened by the larger delay time. Accordingly, the intensity of the Rabi oscillation is weakened. The disappearance of AT splitting in the photoelectron spectra at larger delay time results from the non-sufficient Rabi oscillation. The different Rabi oscillation leads to the different population left in each electronic state, which leads to the periodical change of the populations in the ground state and excited states with the increase of the delay time. The results illustrate that by controlling the delay time, the needed population in the excited state of interest can be obtained, which provides the foundation for realizing the light manipulation of molecular processes.

References

[1] Braun M and Meier C 1996 *J. Chem. Phys.* **105** 530
[2] Miao X Y, Zhang J F and Jia X F 2008 *Europhys. Lett.* **82** 33001
[3] Miao X Y, Wang L and Song H S 2007 *Phys. Rev. A* **75** 042512
[4] Liu R F, Zhai H S, Gao Y L and Liu R Q 2008 *Chin. Phys. Lett.* **25** 2016
[5] Zhao Z Y, Han Y C, Yu J and Cong S L 2014 *J. Chem. Phys.* **140** 044316
[6] Yu J, Wang S M, Yuan K J and Cong S L 2006 *Chin. Phys.* **15** 1996
[7] Ma N, Wang M S, Yang C L, Ma X G and Wang D H 2010 *Chin. Phys. B* **19** 023301
[8] Zhang M, Tang T T and Zhang C M 2014 *Acta Phys. Sin.* **63** 023302 (in Chinese)
[9] Zhang M, Wang M S, Xiong D L and Ma N 2013 *Mol. Phys.* **111** 61
[10] Zhu Y H, Song P and Ma F C 2014 *Braz. J. Phys.* **44** 189
[11] Meng Q T, Yang G H, Sun H L, Han K L and Lou N Q 2003 *Phys. Rev. A* **67** 063202.
[12] Meng Q T, Liu X G, Zhang Q G and Han K L 2005 *Chem. Phys.* **316** 93
[13] Wang J, Liu F, Yue D G, Zhao J, Xu Y, Meng Q T and Liu W K 2010 *Chin. Phys. B* **19** 123301
[14] Cheng W J, Zhang S A, Jia T Q, Feng D H and Sun Z R 2014 *Chin. Phys. Lett.* **31** 053301
[15] Niu Y Y, Wang R and Xiu J L 2012 *Acta Phys. Sin.* **61** 093302 (in Chinese)
[16] Xie Y L, Zhu S D, Liu J, Xiao T H, Feng B H and Li Z Y 2016 *Chin. Phys. B* **25** 044203
[17] Frohnmeyer T and Baumert T 2000 *Appl. Phys. B* **71** 259
[18] Wollenhaupt M, Assion A, Bazhan O, Liese D, Sparpe-Tudoran C and Baumert T 2002 *Appl. Phys. B* **74** S121
[19] Erdmann M, Shen Z and Engel V 2002 *Chem. Phys. Lett.* **351** 275
[20] Yuan K J, Sun Z G, Cong S L, Wang S M, Yu J and Lou N Q 2005 *Chem. Phys.* **316** 245
[21] Yuan K J, Wang S M and Cong S L 2005 *Chin. Phys. Lett.* **22** 2534
[22] Hu W H, Yuan K J, Han Y C, Shu C C and Cong S L 2010 *Inter. J. Quan. Chem.* **110** 1224
[23] Yan T M, Han Y C, Yuan K J and Cong S L 2008 *Chem. Phys.* **348** 39
[24] Hao X, Zhan W S, Wang S, Zai J B and Dai H P 2014 *Laser Phys.* **26** 026001
[25] Jing D, Wang S, Zhan W S, Yang J and Zhang Y D 2017 *Eur. Phys. J. D* **71** 220
[26] Liu Y F, Liu R Q and Ding J X 2009 *Chin. Phys. Lett.* **26** 073301
[27] Liu Y F, Liu R Q and Ding J X 2010 *Chin. Phys. B* **19** 033301
[28] Miao X Y, Wang L, Yao L and Song H S 2006 *Chem. Phys. Lett.* **433** 28
[29] Miao X Y, Li X and Song H S 2008 *Chin. Phys. Lett.* **25** 915
[30] Yao H B and Zheng Y J 2011 *Phys. Chem. Chem. Phys.* **13** 8900
[31] Guo W, Lu X Q, Wang X L and Yao H B 2014 *Phys. Chem. Chem. Phys.* **16** 20755
[32] Guo W, Lu X Q, Wang X L and Yao H B 2015 *Chin. Phys. B* **24** 013302
[33] Brixner T, Krampert G, Pfeifer T, Selle R and Gerber G 2014 *Phys. Rev. Lett.* **92** 208301
[34] Schlesinger M, Mudrich M, Stienkemeier F and Strunz W T 2010 *Chem. Phys. Lett.* **490** 245
[35] Zhang H, Han K L, Zhao Y, He G Z and Lou N Q 1997 *Chem. Phys. Lett.* **271** 204
[36] Chu T S, Zhang Y and Han K L 2006 *Int. Rev. Phys. Chem.* **25** 201
[37] Magnier S, Aubert-Frecon M and Allouche A R 2004 *J. Chem. Phys.* **121** 1771
[38] De Vivie-Riedle R, Kobe K, Man J, Meyer W, Beischl B, Rutz S, Schreiber E and Woste L 1996 *J. Phys. Chem.* **100** 7789
[39] Sun Z G and Lou N Q 2003 *Phys. Rev. Lett.* **91** 023002
[40] Meier C, Engel V and Manthe U 1998 *J. Chem. Phys.* **109** 36